C.U. Shah College of Pharmacy[1], S.N.D.T. Women's University, Santacruz (W), Mumbai 400049, India; Department Pharmaceutics, Biopharmaceutics & NutriCosmetics[2], Insitute of Pharmacy, Freie Universität Berlin, Germany

# Nevirapine nanosuspensions for HIV reservoir targeting

R. Shegokar[1,2], K. K. Singh[1]

*Received October 25, 2010, accepted November 16, 2010*

*Dr. (Mrs.) Kamalinder K. Singh, Principal and Professor of Pharmaceutics, C.U. Shah College of Pharmacy, S.N.D.T. Women's University, Santacruz West, Mumbai, India*
*kksingh35@rediffmail.com*

*Pharmazie 66: 408–415 (2011)* *doi: 10.1691/ph.2011.0317*

In this paper we discuss, production, characterization and *in-vivo* evaluation of nevirapine nanosuspensions. Laser diffraction showed that the average particles size was 457 nm. Following single-dose administration, the plasma gamma concentration profiles showed fast release. Macrophage uptake studies confirmed enhanced cellular uptake for nanonized nevirapine with no added cytotoxicity. Gamma scintigraphy showed that the nanosuspension prepared can be used to target spleen, thymus and lungs, which represent anatomical viral reservoirs. Thus nevirapine nanosuspensions with targeting potential have been prepared successfully.

## 1. Introduction

More than 40 percent of the drugs coming from high-through put screening are poorly soluble in water (Lipinski 2002). Poorly water-soluble drugs show many problems such as too low bioavailability and or erratic absorption. The performance of these drugs is dissolution rate-limited (for Class II and III drugs) and affected by the fed/fasted state of the patient. Dissolution rates of sparingly soluble drugs are related to the particle size as well as shape. The possibility of targeted drug delivery has also provided an opportunity to utilize nanosuspension dosage forms for more complex molecules such as proteins and nucleic acid based drugs (Wong et al. 2008).

A number of formulation approaches were used to resolve the problems of low solubility and low bioavailability. The approaches include micronization, solubilization with co-solvents, use of permeation enhancers, oily solutions, surfactant dispersions, salt formation and precipitation techniques (Junghanns and Müller 2008). These techniques for solubility enhancement have some limitations. Micronization by colloid mills or jet mills increases the dissolution velocity of drug due to increase in surface area but does not increase the saturation solubility (Müller et al. 2001). Nanonization can resolve the problems associated with these conventional formulation approaches. The drug microparticles are transferred to nanoparticles by bottom up or top down technology (Müller et al. 2001) or disintegration methods.

Nanosuspensions (NS) consist of the pure poorly water-soluble sub-micron drug colloidal dispersion stabilized by surfactants (Müller et al. 2000). Nanosuspensions solve the problems associated with delivery of poorly water-soluble drugs and lipid-soluble drugs (Rabinow 2004). Nanosuspensions differ from nanoparticles (Shobha et al. 1999), which are polymeric colloidal carriers of drugs (nanospheres and nanocapsules), and solid-lipid nanoparticles (SLN) (Mehnert and Mäder 2001), which are lipidic carriers of drug. Conventionally the drugs that are insoluble in water but soluble in an oil phase system are formulated in liposomes, emulsion systems but these lipidic formulation approaches are not applicable to all drugs. In these case nanosuspensions are preferred for drugs that are insoluble in both water and in organic media. This formulation approach is most suitable for compounds with high log P value, high melting point and high dose (Patravale et al. 2004). Dissolution of drug is increased due to increase in the surface area of the drug particles from micrometers to the nanometer size. According to Noyes-Whitney equation dissolution velocity increases due to increase in the surface area from micron size to particles of nanometer size. Drugs with poor solubility and low bioavailability are called 'brick dust' candidates. Once abandoned from formulation development work they can be rescued with nanosuspension technology. A nanosuspension not only solves the problems of poor solubility and bioavailability but also alters the pharmacokinetics of drug and thus improves drug safety and efficacy. Therefore decrease in particle size results in an increase in dissolution rate (Mitra and Christer 1995).

Despite the significant impact of antiretroviral therapy (ART), the worldwide human immunodeficiency virus type 1 (HIV-1) pandemic continues to grow (Sharland et al. 1998). Almost all anti-retrovirals have high dose and needs to be administered more than twice a day results in life-long therapy. The targeting potential of some drug delivery systems such as solid lipid nanoparticle, polymeric nanoparticles and nanoemulsions cannot be employed for anti-HIV drugs because of certain limiting factors. Complex dosing regimens, costs, side effects, biodistribution limitations, and variable drug pharmacokinetic patterns have affected the long-term efficacy of antiretroviral medicines. Van Eerdenbrugh et al. (2007) prepared loviride nanosuspensions ($264 \pm 14$ nm/distribution range of $59 \pm 6$ nm) using media milling to improve its dissolution and absorption properties. A Caco-2 experiment on the nanopowder showed a significantly higher cumulative amount transported to cells after 120 min ($1.59 \pm 0.02$ μg) compared to the physical mixture ($0.93 \pm 0.01$ μg) and the untreated loviride ($0.74 \pm 0.03$ μg).

Similarly, Gendelman et al., prepared an indinavir nanoparticle (NP-IDV) formulation packaged into carrier bone marrow-derived macrophages (BMMs). After a single administration,

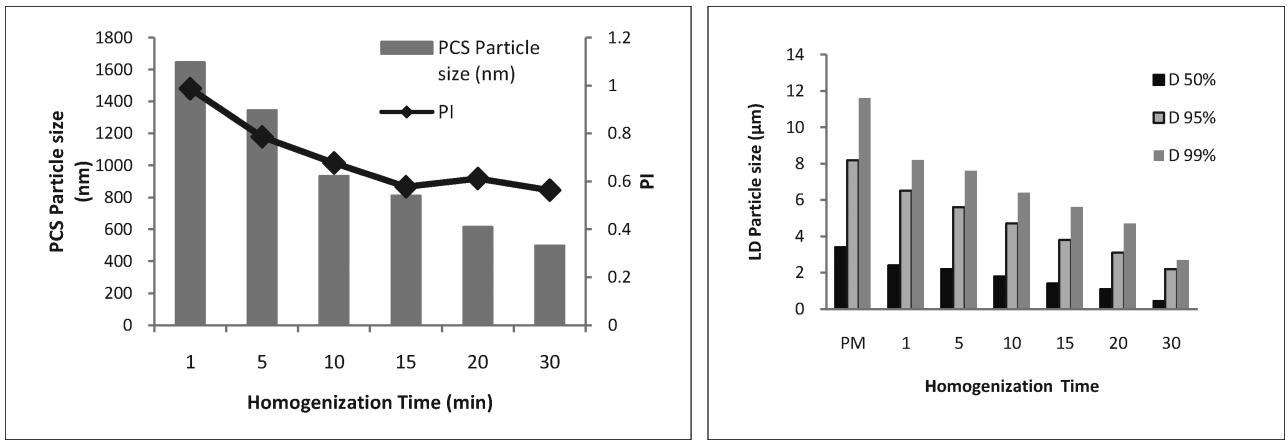


Fig. 1: a) PCS diameters (z-average) and polydispersity indices b) laser diffractometry diameters of nevirapine nanosuspension on the day of production

formulation demonstrated robust lung, liver and spleen drug distribution with IDV levels greater than 50 μM for 2 weeks. NP-IDV-BMMs administered to HIV-1 challenged humanized mice revealed reduced numbers of virus-infected cells in plasma, lymph nodes, spleen, liver, and lung (Dou et al. 2006). P. Wigerinck et al. developed a TMC278 (rilpivirine) nanosuspension which gave sustained plasma levels up to 2 months in rats and as long as 6 months in dogs and humans when applied subcutaneously and intramuscularly. Even after 3 months, the tissue distribution pattern was similar to that previously observed after oral dosing, with 5-fold higher concentrations in lymphoid tissues than in plasma. Typical pharmacokinetic parameters, area under curve showed depot formation after subcutaneous and intramuscular injection. It was observed that the intramuscular route was better tolerated than the subcutaneous one (van't Klooster et al. 2008).

In the present article, a crystalline nanosuspension of nevirapine, was developed for parenteral application to improve the drug loading and to increase targeting potential. The compound has high permeability and low solubility in the gastrointestinal tract, thus fulfilling the criteria for a BCS II compound and hence chosen for the present study. Nanosuspensions of nevirapine were prepared and exploited for their targeting potential to HIV viral reservoirs in the body by carrying out cellular uptake and biodistribution studies.

## 2. Investigations, results and discussion

### *2.1. Preparation and characterization of nevirapine nanosuspension*

The nanosuspensions were white dispersions with pH in a range of $6.85 \pm 0.17$. All the nanosuspension showed excellent syringability and injectability with no sign of clogging or blockage of syringe. Drug content of was found to be $97.63 \pm 1.42\%$.

#### *2.1.1. Particle size analysis and Zeta potential*

Photon correlation spectroscopy (PCS) data showed a mean particle size of $457 \pm 10$ nm for the nanosuspension and a size distribution below 2000 nm (Fig. 1a). The polydispersity index at 90 degree and 20 °C was noted for the nanosuspension and found to be $-0.578 \pm 0.176$ nm confirming formation of a polydispersed phase. It is important to confirm the PCS results by Laser diffractometry (LD) as PCS is a more specific technique for nanometer size range and may not detect particles larger than 3000 nm while LD is more accurate for the micron range particle size and not sensitive to detect very small nanometer particles. Laser Diffractometry (Fig. 1b) revealed that more than 90.0% particles were smaller than $200 \pm 92$ nm, while LD showed 95% particles below $2200 \pm 45$ nm and 99% particles were below $2500 \pm 20$ nm. Both the results from PCS and LD were comparable. The zeta potential tested in miliQ water was –30.23 mV confirmed the stability of system (Kayes 1977). Fig. 2 shows the effect of two variables viz. homogenization pressure and time on particle size. Increase in homogenization pressure showed decrease in particle size.

#### *2.1.2. Atomic Force Microscopy*

Atomic force microscopy (AFM) images of the nanosuspensions were obtained in the non contact mode. Figure. 3 shows the AFM image of nanosuspensions taken within 24 h after deposition. It was possible to observe many agglomerates in nanosuspension, which may be due to multiple layer formation during drying. The topographical changes could be influenced by different factors such as time required for drying, drying condition and formulation composition. The results obtained after AFM imaging have the same magnitude than PCS measurements: a good reproducibility existed between the two techniques (Jacobs. and Mŭller 2002).

#### *2.1.3. XRD Measurements*

The X-ray diffractogram of nevirapine pure drug and nanosuspension is shown in Fig. 4 Drug diffractogram shows distinct peaks 2θ angle of 9.32, 13.12, 13.52, 15.4, 17.24, 19.16, 20.76, 23.2, 25.56, and 26.52 of high intensity where as dried homogenized nanosuspensions showed a decrease in the heights of these high intense peak. Peaks at 19.16 and 25.56 can be seen with very low intensities confirming the amorphous nature of

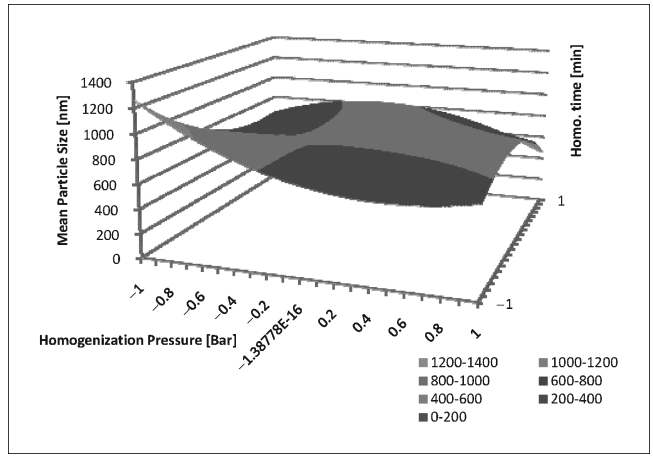


Fig. 2: Response surface graph for NS1 showing effect of homogenization pressure and time on mean particle size

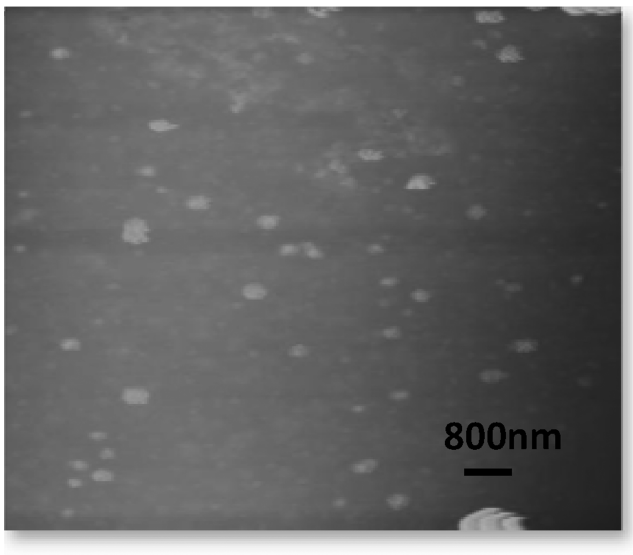


Fig. 3: Atomic force microscopy image of nevirapine nanosuspension

the nanosuspensions. The halo region indicates a small amount of liquid (water) present which could of be any hydrophobic surfactant used in the formulation. Decrease in crystallinity was also reported after nanonization (Mauludin et al. 2009).

### 2.2. Cellular uptake studies

Determination of drug concentration in macrophage cells can provide a rapid, simple and sensitive means to quantify cell-associated nanoparticles. Figure 5 (left) shows the cellular selective uptake of nanosuspensions in primary macrophages. The cellular level of drug increased with time of incubation and the process seemed saturable at high concentrations. Nevirapine drug solution showed a concentration of 1.82 μg/million of cell indicating very fast uptake of the drug by macrophages. Yazdanian and glynn (1998) reported that nevirapine has excellent permeability to brain microvessel endothelial cells and Caco-2 cells. The uptake of nanonized nevirapine suspension in the presence of surfactant showed a 1.57 fold higher drug concentration within 5 min whereas pure drug was not able to follow even after 2 hours of incubation. Nevirapine concentration in macrophages increased over the period of time till 1 h. At end of two hours, a 2.76 fold increase in drug concentration as compared to pure drug was observed. This means that the nanonized drug could cross the cellular barrier and enter very fast in to the cell. This could be due to the particle site of nanosuspensions (457 nm) which is ideal for fast macrophage uptake. The result indicated that the cellular uptake of NS was time dependent. Kayser (2000) reported an enhanced uptake of aphidicolin nanosuspensions in murine macrophages.

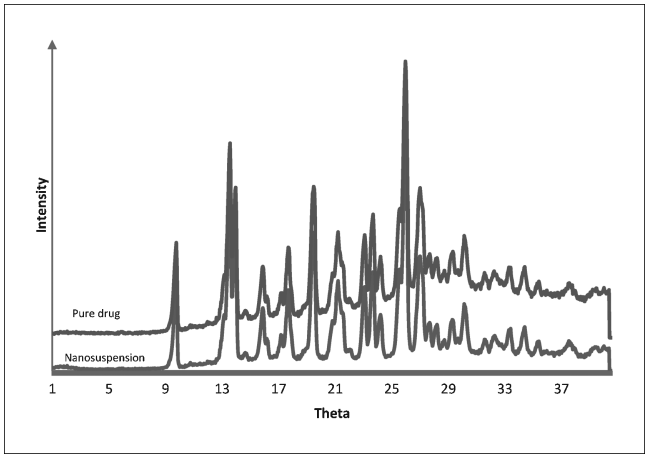


Fig. 4: X-ray diffractogram depicting crystalline state of pure drug and nevirapine nanosuspensions

### 2.3. Cytotoxicity assay

To assess the cytotoxicity of nanosuspensions, a MTT assay was performed. Figure. 5b shows the percent viability of cells after incubation with NVP-DS and NS. At lower concentrations the cell viability was found to be high as the drug concentration was increased up to 2 μg/ml beyond which no change in cell viability was observed. Cell viability showed dose dependent response up to 2 μg/ml. Higher levels of nevirapine concentration in macrophage cells did not cause an increase in cellular cytotoxicity. Thus, it can be seen that both NVP-DS and NS showed inhibition of cells at higher concentration with no added cytotoxicity. Also exposure to higher concentrations of nevirapine resulted in faster cell death. From phagocytic uptake studies, it has been seen that nanosuspensions showed higher cellular uptake than that of pure drug, indicating a higher concentration inside the cell. This suggests that even at higher levels toxicity remained unchanged for nanocarriers. Thus, the developed nevirapine nanosuspensions showed no increase in *in-vitro* cytotoxicity.

### 2.4. In-vivo studies on nevirapine nanosuspensions

Radiolabeling of nevirapine nanosuspension with $99mTcO_4^-$ was successfully optimized. Nevirapine nanosuspensions were directly labeled using $^{99m}TcO_4^-$ and stannous chloride as a reducing agent. The pH (6.5–7), incubation temperature and time of incubation was optimized. An increase in these variables had no marked effect on radiolabeling. The amount of stannous chloride (reducing agent) played a determining role. A high radiolabeling for all nevirapine formulations was achieved at 1000 μg of stannous chloride. A less amount of stannous chloride resulted in poor labeling.

Nevirapine radiolabelled formulations were subjected to *in vitro* stability test in PBS (pH 7.4) and plasma. Formulations showed excellent *in vitro* stability of 84–97% and were stable over the period 24 h with *in-vivo* stability of 90–97%. High binding affinity of $^{99m}Tc$ with hydrophobic surfaces of nanosuspensions was established by challenging the radiolabelled formulations with DTPA at different concentrations of 0.05 to 2%. Low percentages of DTPA does not have much effect on labeling efficiency but at higher concentration of 2% DTPA concentration reduction in radiolabeling efficiency by about 8.02 – 8.50%. This could be due to higher strength and binding affinity of $^{99m}Tc$ with NVP-DS and NS.

#### 2.4.1. Blood clearance

Blood clearance of nevirapine nanosuspensions was investigated. The radioactivity was high enough at 5 min after administration and was negligible after 4 h indicating that nanosuspensions have a significantly long circulation time in the vascular compartment. Gamma $count_{max}$ was noted to be 25.17 within 5 min for NS and maintained blood levels until 8 h but with a very low gamma count of 1.092. The comparative blood clearance profiles of radio labeled complex NVP-DS and NS are shown in Fig. 6. Pure drug was rapidly cleared from blood stream at a 1386.11 ml/h clearance rate.

#### 2.4.2. Gamma scintigraphic imaging

Gamma scintigrams of rats after administration of NVP-DS and NS are shown in Fig. 7. It was observed that free drug

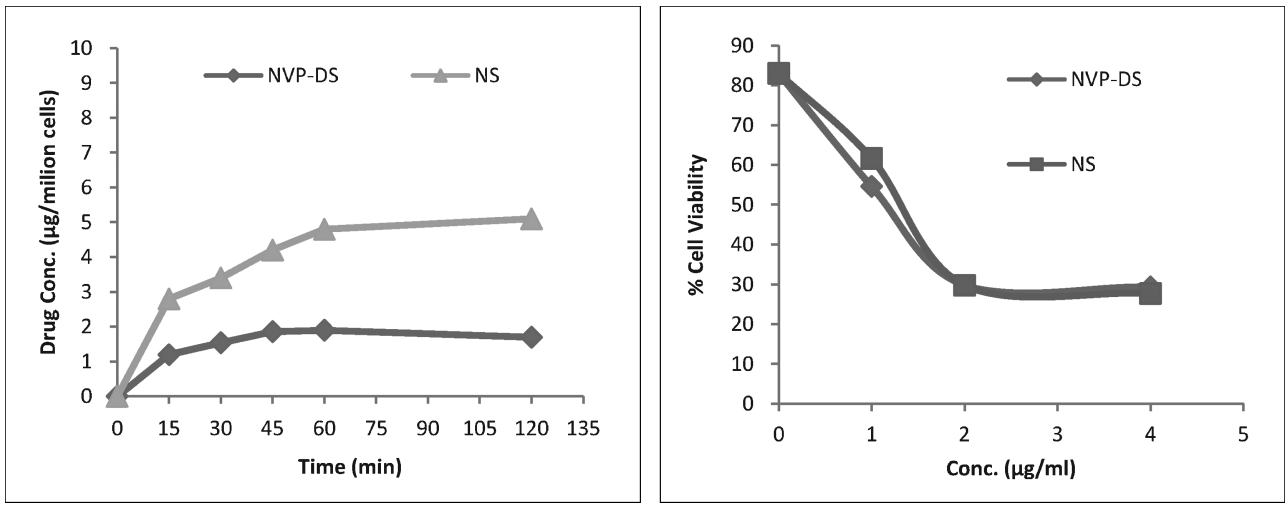


Fig. 5: The percent phagocytosis (left) and cell viability (right) of nevirapine nanosuspensions incubated with macrophages

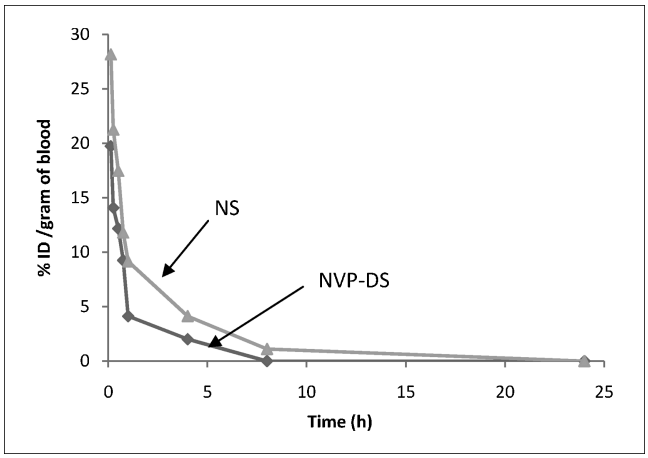


Fig. 6: Comparative blood clearance profile of $^{99m}$Tc NVP-DS and nanosuspension at different time intervals in rats

accumulated maximally in the kidney and bladder indicating its rapid excretion. Entire drug was excreted in less than 24 h in case of NVP-DS. NVP-DS and NS mainly accumulated in RES organs and showed significant radioactivity entering in spleen within 30 min. Nanonisation of nevirapine in the presence of surfactant reduced its excretion through kidney and allowed more deposition in the liver and spleen. The developed nanosuspension formulation contains a large fraction of spherical populations small enough to escape the space of blood vessel and tissue and reaching to hepatocytes or macrophages. The nanosuspension showed comparable accumulation in RES organs. The localization of formulation was more prominent at 1 and 8 h. NVP-DS was completely excreted from the body while NS were able to retain in smaller amounts in RES organs at 24 h. It was observed that free drug was mainly excreted by the kidney and bladder. Nanonisation of nevirapine to a nanosuspension reduced its excretion through kidney concentrating them

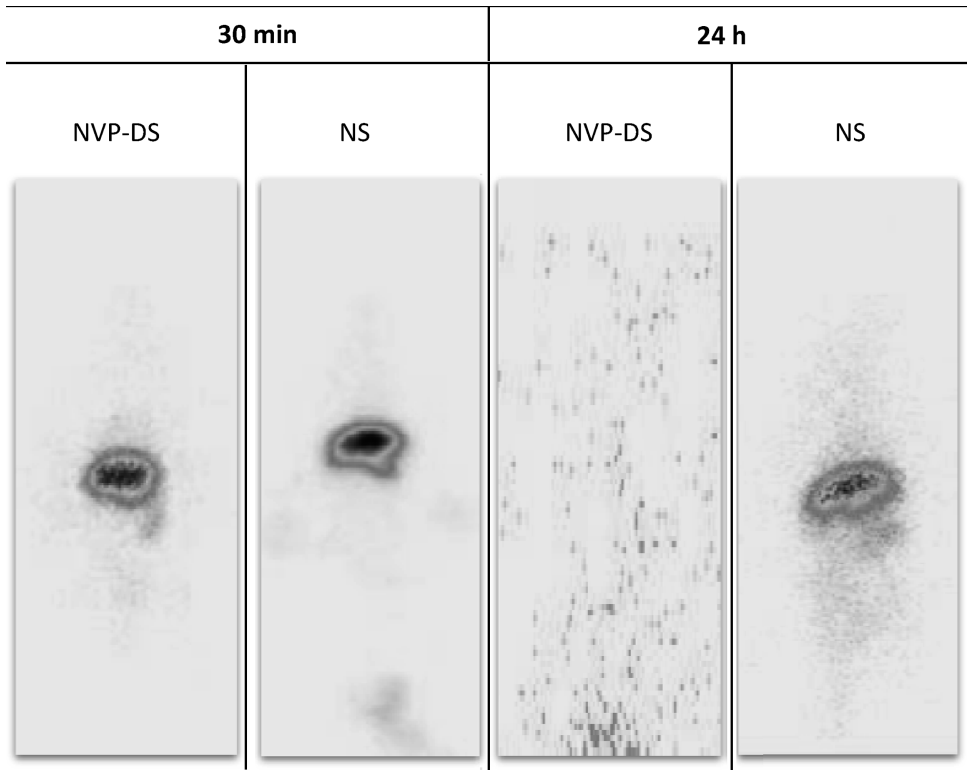


Fig. 7: Gammascintigraphy images of nevirapine drug solution (NVP-DS) and nanosuspensions (NS) after 30 min and 24 hours

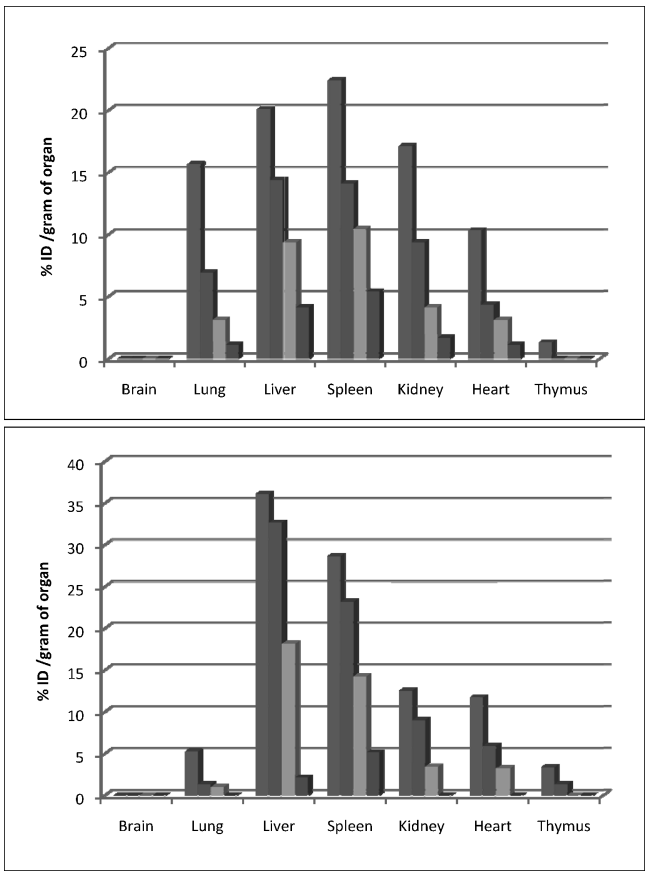


Fig. 8: Radioactivity of NVP-DS (above) and NS (below) in different organs from various experimental group

in the liver and spleen as shown in gammascintigrams. Nevirapine accumulated in various organs especially in the RES systems. The developed nanosuspension contains significant fraction of larger particle population which gets easily phagocytosed by macrophages allowing to enter in hepatic and spleenic circulation. Drug levels were further confirmed by performing biodistribution studies and subjecting organs/of interest to gamma count (Gao et al. 2008).

### *2.4.3. Tissue distribution*

The accumulation of NVP nanosuspensions in various HIV reservoirs was the success of this research. Comparative biodistribution profiles in lung after i.v. administration of radiolabelled NVP-DS and NS are depicted in Fig. 8. Nanosuspensions have demonstrated low lung activity probably attributable to the lack of mechanical filtration by the capillary bed due to negative zeta potential charge of NS (near − 30 mV).

NVP-DS showed $AUC_0^{24}$ of 40.288 counts. h/g and MRT of 4.45 h. Nevirapine nanonized suspensions showed marked reduction in $AUC_0^{24}$ of 25.068 counts. h/g in lungs probably because of their inability of being retained in lungs. However, the MRT of NS was found be comparable with that of NVP-DS. In the heart, nanosuspension showed a slightly higher value for $AUC_0^{24}$ (76.703 counts. h/g) than NVP-DS (66.175 counts.h/g), but MRT for pure drug was observed (10.672 h) to be longer to that of NS (4.781 h). In liver, NS showed $AUC_0^{24}$ of 385 counts. h/g which was much higher than that of NVP-DS which showed lower area under curve. The MRT of NS was found to be higher (7.153 h) than that of pure drug (5.747 h). Pure drug solution showed $AUC_0^{24}$ of 120.253 counts. h/g and MRT of 4.563 h in spleen. NS showed three times higher $AUC_0^{24}$ than NVP-DS with prolonged MRT in spleen (7.153 h).

Significant differences in the biodistribution profiles of NVP-DS and NS were observed. Further, dissection studies estimated that in the liver approximately 46 to 35% of the injected dose was in liver parenchymal cells. Organ biodistribution results indicated that nanosuspension clearance from blood is mainly due to the liver. This phenomenon could be explained by two classically described mechanisms. One is the action of Kupffer cells and other macrophages involved in the nanoparticles capture (Barratt 2000). The high liver uptake might also have been due to the high hydrophobicity of the compound. $AUC_0^{24}$ was noted to be lowest for NVP-DS i.e. 217.485 counts. h/g. The clearance rate was much higher for pure drug solution than that of nanosuspension. The total radioactivity associated with the blood and collected organs at the end of the experiment were approximately 80% of the total injected dose. Thymus, as it is an important organ in regulating T cell maturation, has an important role in diseases related to the immune system. NVP-DS and NS showed successful accumulation in thymus but with lower gamma count. The main objective of the drug delivery system was to facilitate phagocytosis and target spleen as it plays important role in HIV/AIDS. The developed nanosuspension was able to successfully target the spleen. At all time intervals higher values of F were observed than the tabulated values. This indicated that at 95 % confidence limit ($p = 0.05$), the differences of mean gamma count between various tissues were highly significant. The *F*-ratio obtained for nevirapine drug solutions also showed significant differences of mean with a maximum difference at 60 min. ANOVA concluded that all groups have significant differences. Similarly various time intervals of the nevirapine experimental group have higher values of F than the tabulated value (>2.85). This indicated that at 95% confidence limit ($p = 0.05$), the differences of mean gamma count between various tissues were significantly different. The *F*-ratio obtained for nevirapine drug solutions also showed significant differences of mean with the maximum difference at 30 min. ANOVA further confirmed that all groups have significant differences.

Biodistribution studies revealed improved antiretroviral drug accumulation of nanosuspensions as compared to the plain drug solution in various organs of rats when administered as nanosuspension. Higher MRT values in liver and spleen as compared to pure drug solution ensured enhanced bioavailability and prolonged residence of the drug at the target site when given as nanosuspension.

## *2.5. Conclusions*

Stable fast dissolving nevirapine nanosuspensions were successfully prepared using the cold high pressure homogenization technique. AFM confirmed the irregular shape of nanosuspensions. *In-vitro* cellular uptake studies showed enhanced cellular uptake. After intravenous administration, nanosuspensions mainly accumulated in MPS rich organs showed prolonged residence in lymphatic circulation. Higher MRT values in liver and spleen as compared to pure drug solution ensured enhanced bioavailability and prolonged residence of the drug at the target site. Thus, the developed nanocarriers have targeting potential to various vital organs which serve as active and latent reservoirs during HIV infection. Thus, nevirapine nanosuspensions open a new opportunity for improving compliance and for development of HIV chemotherapy by targeting drug at a cellular level without added toxicity.

## 3. Experimental

Nevirapine, a non-nucleoside reverse transcriptase inhibitor (NNRTI) of pharmaceutical grade purity was procured as a gift sample from Alkem

Laboratories, Mumbai, India. Poloxamer 188 (BASF GmbH), Tween 80 (Uniquema, Belgium), Plasdone (Croda Inc.), Polyvinyl pyrollidone (Signet Chemical Corporation, India) were received as gift samples. RPMI (Roswell Park Memorial Institute) medium, fetal calf serum (FCS), dimethyl sulfoxide (DMSO), yellow MTT (3-(4,5-dimethylthiazol-2-yl)-2,5-diphenyltetrazolium bromide, a tetrazole), DMEM (Dulbecco's modified Eagle's Medium), acid propanol phosphate buffer saline (PBS), Hanks buffered salt solution (HBSS), fluid thioglycollate medium, Dulbecco's modified Eagle medium (DMEM), Hypotonic saline (0.18−0.3% NaCl), diethylene triamine pentaacetic acid (DTPA), sodium citrate and stannous chloride were purchased from S.D. Fine Chemicals, Mumbai.

### 3.1. Preparation of nanosuspensions

Aqueous nanosuspensions of nevirapine were produced with a High pressure homogenization technique (Avestin Emulsifex® C50) in continuous mode for 30 min. In-short, nevirapine 2.0% (w/v) powder was dispersed in 2.8% (w/v) of surfactant solution and pre-mixing was performed with high shear Remi over head stirrer followed by Ultra Turrax T25 equipped with rotor (Jahnke & Kunkel, Staufen, Germany) for 1 min at 9500 rpm. The presuspension was homogenized at different pressures for 30 min. A continuous cooling via heat exchanger was used during the whole process to maintain the product temperature between 0 °C and 4 °C. Sampling was done after each time point and characterized for mean particle size and particle size distribution.

### 3.2. Characterization of nanosuspensions

#### 3.2.1. Resuspendability

Prepared nanosuspensions were poured in 100 ml measuring cylinder and allowed to sediment for 24 h and redispersed again. The total number of strokes to redisperse nanosuspensions was counted.

#### 3.2.2. Syringability

The syringability of the nanosuspensions was determined and expressed as the time needed to completely fill a 10 ml syringe, equipped with a 40 mm needle with diameter of 21 G (0.8 mm).

#### 3.2.3. Injectability

The injectability was determined using a 5 ml syringe, the plunger was slowly moved so as to eject the suspension through the needle was qualitatively determined by assessing the pressure required to eject the contents from the syringe.

#### 3.2.4. Drug content

Total drug content of nanosuspensions was carried out using liquid-liquid extraction. One milliliter of sample was added in 10 ml of chloroform and extracted against 0.1N HCl. The clear aqueous portion were analyzed spectrophotometrically at 313 nm. The amount of drug was calculated from the standard curve equation.

### 3.3. Particle size determination

#### 3.3.1. Photon correlation spectroscopy (PCS)

PCS was performed on nanosuspension in double distilled water using the Beckman particle size analyser N5 at 90° angle at 25 °C temperature. The analysis yields the mean diameter of the bulk population and the polydispersity index of nanosuspensions.

#### 3.3.2. Laser diffractometry (LD)

LD analysis was carried out using a Mastersizer 2000 (Malvern Instruments, UK) in deionized water as dispersion medium. The instrument was operated with the Hydro S sample dispersion unit. LD yields volume weighted diameters d(v)50%, d(v)90%, d(v)95% and d(v)99%.

#### 3.3.3. Atomic Force Microscopy measurements (AFM)

AFM measurements were performed on freshly prepared nevirapine nanosuspensions. A silanized mica was prepared by dropping 0.1% of 3-aminopropyltriethoxysilane (APTES) solution onto a mica surface. After storing it for 30 min at room temperature, excess amount of APTES was washed with water. The sample was diluted in water (1:100) and 40 µl was deposited onto a small mica disk with a diameter of 1 cm. After 2 min, the excess of sample was removed using paper filter. The microscopy images were obtained using the Veeco Digital Instruments Multimode Nanoscope IV (Tapping mode AFM, Cantilever: Silicon nitride (spring constant 30–80 N/m; resonance freq. ~340 kHz). ProScan Data Acquisition software developed under Windows 95.

#### 3.3.4. X-Ray diffraction Studies (XRD)

A Diffraction study was performed on coarse drug and nanosuspension at room temperature with a Philips X-ray Generator PW 1830 from Philips (Amelo, Netherlands). The diffraction pattern was measured at a voltage of 40 kV and a current of 40 mA in the 2θ-region of 4 °C–60 °C. The sample was rotated during measurement at 1 rotation/s to allow better reproducibility of the measured intensities.

#### 3.3.5. Zeta potential measurements

The surface charge on particles was assessed by diluting sample in MiliQ water using a Brookhaven Zeta PALS, BI-ZETAMAN, Ver. 1.

### 3.4. Phagocytic uptake studies

Macrophage uptake of developed nanosuspensions was carried out in peritoneal macrophage cells harvested from male Wister rat (180–220 g) by intraperitoneally injecting thioglycollate medium Mosqueira et al. 2001. The rats were deeply anesthetized by ether and on 3rd day 10 ml of freshly prepared HBSS was injected in peritoneal cavity. After 3 min gentle message the abdomen was cut opened and HBSS was recovered. The lavaged cell suspension was centrifuged at 1300 rpm at 4 °C, and the pellet was resuspended in HBSS. Peritoneal macrophage cells were then cultured in sterilized culture plates containing glass cover slips with seeding density of $1 \times 10^6$ cells/ml with RPMI1640 medium supplemented with 10% fetal bovine serum and incubated at 37 °C ± 2 °C at 5% $CO_2$ for 24 h to form a confluent monolayer. After three hours of incubation macrophages were washed and rinsed twice with HBSS to remove the non-adherent cells. Monolayer formation was checked under a light microscope.

The cellular uptake of nanosuspensions was initiated by exchanging the transport medium with freshly prepared nevirapine nanosuspensions at 37 ± 2 °C. In each culture well, 250 ml of pure drug solution (NVP-DS) and nanosuspension (NS) were added. The PBS (pH 7.4) solution added to cultured macrophages treated as control. At specified times intervals of 15, 30, 45, 60 and 120 min, the phagocytosis was terminated by immersing the plate in an ice bath. The cells were separated from the medium by centrifuging at 2000 rpm, 15 min (Sorvall Biofuge Primo R centrifuge, Thermo Electron Corporation, India) and the supernatant was collected. The cells were further lysed using hypotonic solution and centrifuged at 10,000 rpm. The absorbance associated with the nanosuspensions harvested cells and supernatant was determined using UV spectrophotometer (UV Visible Double Beam Spectrophoometer, 2201, Systronics, India) at 313 nm. The percent cellular uptake was calculated using the following formula. The experiment was run in triplicate for each formulation. The results were expressed as the mean ± SD.

$$\text{Uptake efficiency}\,(\%) = (\text{W sample}/\text{W total}) \times 100 \quad (1)$$

where $W_{sample}$ is the amount of drug associated with macrophage cells and W total is the total amount of drug in the feed nanosuspension.

### 3.5. Cytotoxicity studies

Cytotoxicity on nevirapine nanosuspensions were determined in a J774.A12 murine macrophage cell line using a MTT cytotoxicity assay. NVP-DS was considered as standard. The study was carried out at three different doses 1, 2 and 4 µg/ml for nevirapine nanosuspensions. Appropriate dilutions of the test formulations were made prior to administration in order to deliver the selected doses. J774A-1 murine macrophages were seeded in density of $1 \times 10^5$ in 96 flat well bottom culture plates containing 200 µl of DMEM and incubated overnight. The cells were suspended in RPMI with 10% FCS, 100 U of penicillin/ml and 100 µg of streptomycin/ml at 37 ± 2 °C in humidified incubator with 5% $CO_2$ (Forma Scientific Inc., Marjetta, OH, USA). After overnight culture, the cells were washed thrice with DMEM and then a mixture of 80 µl of fresh DMEM and 20 µl of the respective drug concentrations was added to each cell. After 24 h treatment, 10 µl of 2 mg/ml MTT solution was added to culture plates and incubated for 6 h at 37 ± 2 °C. At the end of 6 h, the MTT reaction was terminated by addition of acid propanol (1 M HCl: isopropanol in 1:24 ratio). At the end of the incubation period, the medium was removed and the converted dye was solubilized in acidic propanol. Absorbance of converted dye was measured spectrophotometrically at 570 nm. The percent cytotoxicity was calculated for all the experiments and reported as mean of three. The results were expressed as

**Table 1: Quality control check of radiolabelled $^{99m}$Tc-nanosuspension complexes**

| T(h) | *In-vitro* stability | | | | *In-vivo* stability | |
|---|---|---|---|---|---|---|
| | PBS | | plasma | | | |
| | NVP-DS | NS | NVP-DS | NS | NVP-DS | NS |
| 0.5 | 96.63 ± 2.41 | 95.22 ± 2.53 | 94.62 ± 1.88 | 94.68 ± 1.62 | 96.15 ± 1.20 | 95.75 ± 1.32 |
| 1 | 95.22 ± 1.83 | 95.23 ± 1.76 | 94.82 ± 1.51 | 94.65 ± 1.11 | 95.67 ± 1.80 | 95.32 ± 1.82 |
| 4 | 93.16 ± 2.40 | 91.01 ± 1.29 | 90.83 ± 1.45 | 93.75 ± 1.35 | 93.81 ± 1.42 | 92.68 ± 1.52 |
| 8 | 89.24 ± 2.13 | 88.15 ± 2.03 | 88.77 ± 1.55 | 91.82 ± 2.12 | 91.88 ± 1.72 | 92.72 ± 1.72 |
| 24 | 84.68 ± 1.72 | 84.28 ± 2.12 | 88.62 ± 0.99 | 87.81 ± 1.75 | 90.67 ± 1.35 | 90.78 ± 1.08 |

the mean ± SD.

$$\text{Cytotoxicity}\,(\%) = \frac{(100 - (Optical\ Density)PBS)}{(Optical\ Density)PBS - (Optical\ Density)Test} \times 100 \quad (2)$$

### 3.6. Radioactive material - Technetium 99m ($^{99m}$Tc)

$^{99m}$Tc was obtained by separation from the parent molybdenum ($^{99m}$Mo) by alumina column solvent extraction technetium generator (B.R.I.T.), Mumbai. NVP-DS and NS was labeled with $^{99m}$Tc by direct labeling method using stannous chloride ($SnCl_2$) as a reducing agent. In short, the $^{99m}$Tc (~1.2 mCi) was mixed with 0.1 ml of stannous chloride solution in 0.1N HCL to reduce the technetium. The pH of solution was adjusted to 6.9–7.1 using Tris buffer. To this mixture, 1 ml of NVP-DS or NS was added and incubated for 30 min at room temperature on mechanical shaker. The labeling efficiency was checked by performing by thin layer chromatography (TLC).

### 3.7. Determination of radiolabeling efficiency

Labeling efficiency of the purified radio labeled formulations was determined by (TLC) using silica gel (SG)-coated fiber sheets of approximately 10 cm in length (Gelman Science Inc., Ann Arber, MI, USA). The TLC was performed using 100% acetone as the mobile phase. A tiny drop (2–3 µl) of the radiolabelled formulation was applied at a point of 1 cm from one end of an TLC-SG strip. The strip was developed in acetone and the solvent front was allowed to reach approximately 8 cm from the origin. The strip was cut into two (1/3, 2/3) halves and the radioactivity in each segment was determined in a well-type gamma-ray counter (Gamma-ray scintillation counter, Type CRS 23C, Electronics Corporation of India Ltd., Mumbai, India). Percent labeling efficiency was calculated from the following formulae:

$$\text{Radiolabeling efficiency}\,(\%) = \frac{\text{LE}}{\text{UE} + \text{LE}} \times 100$$

where LE: count at lower end (one third portion) of TLC plateUE: count at upper end (two third portion) of TLC plate

### 3.8. Stability studies of the nanocarriers-$^{99m}$Tc complex

#### 3.8.1. In vitro stability in PBS

For the determination of *in vitro* stability of all $^{99m}$Tc - NVP-DS or NS complex, 100 µl of the labeled formulation was mixed with 2.0 ml of PBS (pH 7.4) and incubated at room temperature and change in labeling efficiency was monitored over a period of 24 h by TLC.

**Table 2: Enhancement of gamma count obtained by NS over NVP-DS**

| Time [h] | Enhancement in gamma count | | | |
|---|---|---|---|---|
| | Blood | Liver | Spleen | Thymus |
| 1 | 2.22 | 1.80 | 1.28 | 2.59 |
| 4 | 2.05 | 2.27 | 1.64 | 1.35 |
| 8 | – | 1.94 | 1.36 | – |
| 24 | – | 0.51 | 0.95 | – |

#### 3.8.2. In vitro stability in plasma

All $^{99m}$Tc-NS complex (~1.2 mCi) were mixed and incubated at 37 ± 1 °C in human plasma. TLC was performed time to time and checked for dissociation of free technetium from complex.

#### 3.8.3. Transchelation of complexes

The stability and strength of complexation of $^{99m}$Tc- NVP-DS and NS was challenged against various concentrations (0.05%, 0.5%, 1% and 2% w/w) of diethylene triamine penta acetic acid (DTPA) and incubated for 2 h at 37 ± 2 °C. The effect of DTPA on labeling efficiency was measured on TLC using 100% acetone as the mobile phase which allowed the separation of free pertechnetate and DTPA-complex (Rf = 0.8–1.0).

#### 3.8.4. In vivo stability of the labeled complexes

The study was performed in healthy Wister rats. Animals were injected (1.2 mCi), $^{99m}$Tc labeled formulations through the tail vein. The blood was withdrawn through the retro orbital vein at different periodic intervals and spotted on the TLC strips. The TLC was carried out as described previously to estimate the separation of free $^{99m}$Tc/degradation of complex.

### 3.9. In-vivo studies on nevirapine nanosuspensions

#### 3.9.1. Blood kinetics

Rats were anesthetized with an intraperitoneal injection of ~30 µl a mixture 1:1 of ketamine and xylazine. The bolus intravenous injections (BDTM

**Table 3: Pharmacokinetic parameters of nevirapine after intravenous administration in different experimental groups**

| Tissue | NVP-DS | | | NS | | |
|---|---|---|---|---|---|---|
| | $AUC_0{}^{24}$ | $AUMC^0{}_{24}$ | MRT (h) | $AUC_0{}^{24}$ | $AUMC^0{}_{24}$ | MRT (h) |
| | Counts.h/g | | | Counts.h/g | | |
| Blood | 20.483 | 22.965 | 1.306 | 35.893 | 45.316 | 1.959 |
| Lymph | 23.836 | 36.778 | 1.824 | 30.081 | 61.611 | 2.23 |
| Brain | – | – | – | – | – | – |
| Lungs | 40.288 | 179.212 | 4.45 | 25.068 | 108.13 | 4.317 |
| Liver | 217.485 | 1788.08 | 5.747 | 385.0 | 2390.14 | 7.153 |
| Spleen | 120.253 | 548.59 | 4.563 | 307.305 | 2426.26 | 13.468 |
| Kidneys | 121.71 | 817.72 | 9.096 | 90.921 | 425.32 | 4.678 |
| Heart | 66.175 | 469.8 | 10.672 | 76.703 | 366.652 | 4.781 |
| Thymus | 2.743 | 3.732 | 1.544 | 11.573 | 26.632 | 2.304 |

Micro-Fin syringe, insulin type (29 G)) of freshly prepared (36 mg/ml) radio labeled 1.2 mCi NVP-DS and NS were administered via the tail vein. After administration blood was collected from retro-orbital puncture using a fine glass capillary into a small glass test tube containing 0.3% w/w sodium citrate solution at stipulated time intervals of 5, 15, 30, 45 min, 1, 4, 8 and 24 h.

#### *3.9.2. Gamma Scintigraphy imaging*

After administration of radiolabelled nanosuspension of nevirapine noninvasive whole body planar imaging was performed using a Millennium MPS Gamma camera system. Imaging was performed by positioning rats under gamma camera auto tuned to detect the 140 keV radiation of $^{99m}$Tc at 0.5, 1, 2, 4, 8 and 24 h.

#### *3.9.3. Biodistribution studies by post-mortem assessment*

Freshly prepared radiolabelled NVP-DS and nanosuspensions of nevirapine were administered to the respective anesthetized experimental group by bolus intravenous injections. The animals in each of the experimental groups were humanely sacrificed at predetermined time intervals of 1, 4, 8 and 24 h. Major tissues like brain, lung, liver, kidney, spleen, heart and thymus were removed and washed with Ringer's solution. The organs were weighed and a homogenate was prepared. Radioactivity per gram of organ was measured using a well-type gamma scintillation counter.

Acknowledgements: The authors thank the All India Council of Technical Education (AICTE) for financial support the and Bombay Veterinary college for providing facility for carrying out Gammascintigraphy studies.

## References

Barratt GM (2000) Therapeutic applications of colloidal drug carriers. Pharm Sci Technol Today 3: 163–171.

Dou H, Destache CJ, Morehead JR, Mosley RL, Boska MD, Kingsley J, Gorantla S, Poluektova L, Nelson JA, Chaubal M, Werling J, Kipp J, Rabinow BE, Gendelman HE (2006) Development of a macrophage-based nanoparticle platform for antiretroviral drug delivery. Blood 108: 2827–2835.

Gao L, Zhang D, Chen M, Duan C, Dai W, Jia L, Zhao W (2008) Studies on pharmacokinetics and tissue distribution of oridonin nanosuspensions. Int J Pharm 355: 321–327.

Jacobs C, Müller RH (2002) Production and characterization of a budesonide nanosuspension for pulmonary administration. Pharm Res 19: 189–194.

Junghanns JU, Müller RH (2008) Nanocrystal technology, drug delivery and clinical applications. Int J Nanomed 3: 295–309.

Kayes JB (1977) Pharmaceutical suspensions: relation between zeta potential, sedimentation volume and suspension stability. J Pharm Pharmacol 29: 199–204.

Kayser O (2000) Nanosuspensions for the formulation of aphidicolin to improve drug targeting effects against leishmania infected macrophages. Int J Pharm 196: 253–256.

Lipinski C (2002) Poor aqueous solubility- an industry wide problem in drug discovery. Am. Pharm Rev 5: 82–85.

Mauludin R, Müller RH, Keck CM (2009) Kinetic solubility and dissolution velocity of rutin nanocrystals. Eur J Pharm Sci 36: 502–510.

Mehnert W, Mäder K (2001) Solid lipid nanoparticles: production, characterization and applications. Adv Drug Deliv Rev 47: 165–196.

Mitra M, Christer N (1995) The effect of particle size and shape on the surface specific dissolution rate of microsized practically insoluble drugs. Int J Pharm 122: 35–47.

Mosqueira VCF, Legrand P, Gulik A, Bourdon O, Gref R, Labarre D, Barratt G (2001) Relationship between complement activation, cellular uptake and surface physicochemical aspects of novel PEG-modified nanocapsules. Biomaterials 22: 2967–2979.

Müller RH, Jacobs C, Kayser O (2001) Nanosuspensions as particulate drug formulations in therapy. Rationale for development and what we can expect for the future. Adv Drug Deliv Rev 47: 3–19.

Müller RH, Dingler A, Schneppe T, Gohla S (2000) Large scale production of solid lipid nanoparticles (SLN$^{TM}$) and nanosuspensions (DissoCubes$^{TM}$).In: Wise D (ed.) Handbook of Pharmaceutical Controlled Release Technology. New York, Marcel Dekker Inc, pp. 359–376.

Patravale VB, Date AA, Kulkarni RM (2004) Nanosuspensions: a promising drug delivery strategy. J Pharm Pharmacol 56: 827–840.

Rabinow BE (2004) Nanosuspensions in drug delivery. Nat Rev Drug Discov 3: 785–796.

Sharland M, Watkins AM, Dalgleish AG, Cammack N, Westby M (1998) Immune reconstitution in HAART-treated children with AIDS. Highly Active Anti-Retroviral Therapy. Lancet 352: 577–578.

Shobha R., Hiremath R, Hota A (1999) Nanoparticles as drug delivery systems. Ind J Pharm Sci 61: 69–75.

Van Eerdenbrugh B, Froyen L, Martens JA, Blaton N, Augustijns P, Brewster M, Van den Mooter G (2007) Characterization of physico-chemical properties and pharmaceutical performance of sucrose co-freeze-dried solid nanoparticulate powders of the anti-HIV agent loviride prepared by media milling. Int J Pharm 338: 198–206.

van't Klooster, R Verloes, L Baert, F van Velsen, M P Bouche, K Spittaels, J Leempoels, P Williams, G Kraus, Wigerinck P (2008) Long-acting tmc278, a parenteral depot formulation delivering therapeutic nnrti concentrations in preclinical and clinical settings. Conf Retrovir Opportunistic Infect, Feb 3–6: 15.(abstract no. 134).

Wong J, Brugger A, Khare A, Chaubal M, Papadopoulos P, Rabinow B, Kipp J, Ning J (2008) Suspensions for intravenous (IV) injection: a review of development, preclinical and clinical aspects. Adv Drug Deliv Rev 60: 939–954.

Yazdanian M, Glynn SL (1998) Nevirapine has excellent blood brain barrier permeability and absorption properties compared to other HIV antiretrovirals. Int. Conf. AIDS 1016 [abstract no. 60086].